

Structural studies on Te-rich Ge–Te melts

This article has been downloaded from IOPscience. Please scroll down to see the full text article.

2006 J. Phys.: Condens. Matter 18 2749

(<http://iopscience.iop.org/0953-8984/18/10/001>)

View [the table of contents for this issue](#), or go to the [journal homepage](#) for more

Download details:

IP Address: 129.252.86.83

The article was downloaded on 28/05/2010 at 09:05

Please note that [terms and conditions apply](#).

Structural studies on Te-rich Ge–Te melts

I Kaban^{1,4}, P Jónvári², W Hoyer¹, R G Delaplane³ and A Wannberg³

¹ Chemnitz University of Technology, Institute of Physics, D-09107 Chemnitz, Germany

² Research Institute for Solid State Physics and Optics, H-1525 Budapest, POB 49, Hungary

³ The Studsvik Neutron Research Laboratory, Uppsala University, S-61182 Uppsala, Sweden

E-mail: ivan.kaban@physik.tu-chemnitz.de

Received 1 October 2005, in final form 8 December 2005

Published 20 February 2006

Online at stacks.iop.org/JPhysCM/18/2749

Abstract

The structure of liquid Ge₁₅Te₈₅, Ge₂₅Te₇₅ and Ge₃₃Te₆₇ alloys has been studied by neutron and x-ray diffraction. Datasets obtained by the two techniques have been modelled simultaneously with the reverse Monte Carlo simulation method. As a result, the first coordination numbers and nearest neighbour distances for the studied alloys were estimated. On the basis of the experimental data, Ge–Ge bonding appears to be present in liquid Ge₂₅Te₇₅ and Ge₃₃Te₆₇. It has been found that temperature dependences of the physico-chemical properties correlate with the structural changes in liquid Ge₁₅Te₈₅.

1. Introduction

It was established long ago that liquid chalcogens and many binary chalcogenides exhibit anomalous temperature and composition dependences of various physical properties in the liquid state [1–3]. Among them is the Ge–Te system, which is characterized by one congruently melting compound GeTe ($\vartheta_{\text{melt}} = 725\text{ °C}$) and two eutectics at 49.85 at.% Te ($\vartheta_{\text{eut}} = 720\text{ °C}$) and 85 at.% Te ($\vartheta_{\text{eut}} = 375\text{ °C}$), respectively [4, 5]. In addition, a phase with the stoichiometry GeTe₄ was found by crystallization of amorphous alloys around the Ge₂₀Te₈₀ composition [6].

Proceeding from the assumption that the physical properties of the liquid alloys are closely related to the topological and chemical short-range order (SRO), the anomalous behaviour of the physical properties of the Ge–Te melts has been explained by the existence of some structural units (clusters) and by the structural changes occurring with variation of temperature or composition (e.g. [7–12]). However, due to the fact that various physical properties showed the anomalies (maxima and minima) at different compositions, quite different structural models and the existence of various structural units in the liquid Ge–Te alloys have been suggested.

For example, a maximum on the composition dependences of the electrical resistivity and thermoelectric power observed at around 67 at.% Te by Valiant and Faber [7] was interpreted as an indication of the existence of GeTe₂ compound in the liquid phase. Tsuchiya has assumed

⁴ Author to whom any correspondence should be addressed.

the existence of molecular associations with the stoichiometry Ge_1Te_6 after analysis of the temperature and composition dependences of the specific heat, isothermal compressibility, density and thermal expansion of the Te-rich Ge–Te alloys [8, 9].

The liquid eutectic alloy $\text{Ge}_{15}\text{Te}_{85}$ shows interesting temperature-dependent features. Tschirner *et al* [10, 11] found that the electrical resistivity decreases by nearly two orders of magnitude within 100 °C above the eutectic temperature. Herwig and Wobst [12] observed that the temperature dependences of the dynamic viscosity for Te-rich Ge–Te melts show positive deviations from the Arrhenius plot below ~ 525 °C and the activation energy of viscous flow for liquid $\text{Ge}_{15}\text{Te}_{85}$ increases appreciably with decreasing temperature close to ϑ_{eut} . Terzieff *et al* [13] observed a minimum of the magnetic susceptibility at the $\text{Ge}_{15}\text{Te}_{85}$ composition, which disappears at temperatures about 100 °C above ϑ_{eut} . These results have been interpreted in terms of some ‘clusters of atoms’, which exist after melting and disappear when the temperature is 100–150 °C above the eutectic point.

The atomic structure of liquid Ge–Te alloys has been studied in a number of diffraction measurements so far. Neumann *et al* [14, 15] combined neutron and x-ray scattering data for molten $\text{Ge}_{15}\text{Te}_{85}$ and determined the partial correlation functions for Te–Te and Ge–Te pairs up to 600 °C. They assumed that the low temperature melt is built up from pure Te regions and α -GeTe-like clusters, and the locally ordered regions are destroyed with increasing temperature.

Based on the analysis of the neutron weighted total pair correlation function, Nicotera *et al* [16] concluded that the structure of the liquid $\text{Ge}_{17.5}\text{Te}_{82.5}$ alloy can be represented by a model with fourfold coordinated Ge atoms and threefold coordinated Te atoms.

Kameda *et al* [17] assumed that there exists a chemical order in Te-rich Ge–Te liquid alloys based on the bonding between Ge and Te atoms, but the bonding and local atomic order in liquid, amorphous and crystalline states are significantly different in their opinion. Yoshioka *et al* [18] carried out neutron diffraction and EXAFS measurements on liquid $\text{Ge}_{15}\text{Te}_{85}$ and assumed that the bonding state between Ge and Te decreases and becomes weak with increasing temperature. It has been suggested that a strong temperature dependence of the properties of the $\text{Ge}_{15}\text{Te}_{85}$ melt may be explained as a transition from covalent to ionic character of the Ge–Te bonding.

Bichara, Bergman *et al* [19, 20] related the anomalous temperature dependence of the density of liquid $\text{Ge}_{15}\text{Te}_{85}$ to a reorganization of the first coordination shell and interpreted this as a gradual change from a Peierls distorted to a less Peierls distorted structure. It has been suggested that the structural changes undergone by $\text{Ge}_{15}\text{Te}_{85}$ melt mainly consist in an increase of Te neighbours around Ge.

In this work we performed x-ray and neutron diffraction measurements on the liquid alloys $\text{Ge}_{15}\text{Te}_{85}$, $\text{Ge}_{25}\text{Te}_{75}$ and $\text{Ge}_{33}\text{Te}_{67}$. The experimental data are simulated with the reverse Monte Carlo (RMC) technique [21, 22] and the partial structure factors and pair distribution functions obtained are analysed.

2. Experimental procedure

The Ge–Te alloys were prepared from germanium and tellurium pieces of high purity (99.999%) by melting at 800 °C in evacuated and sealed quartz ampoules.

Neutron diffraction experiments were carried out with the liquid and amorphous materials diffractometer SLAD at NFL, Studsvik [23]. The samples were filled into quartz glass capillaries (6 mm diameter and 0.2 mm wall thickness) and sealed under vacuum. The incident wavelength of neutrons was 1.116 Å. The measurements have been performed in the Q -range between 0.4 and 10.4 Å⁻¹. Structure factors were obtained from the scattering intensities after

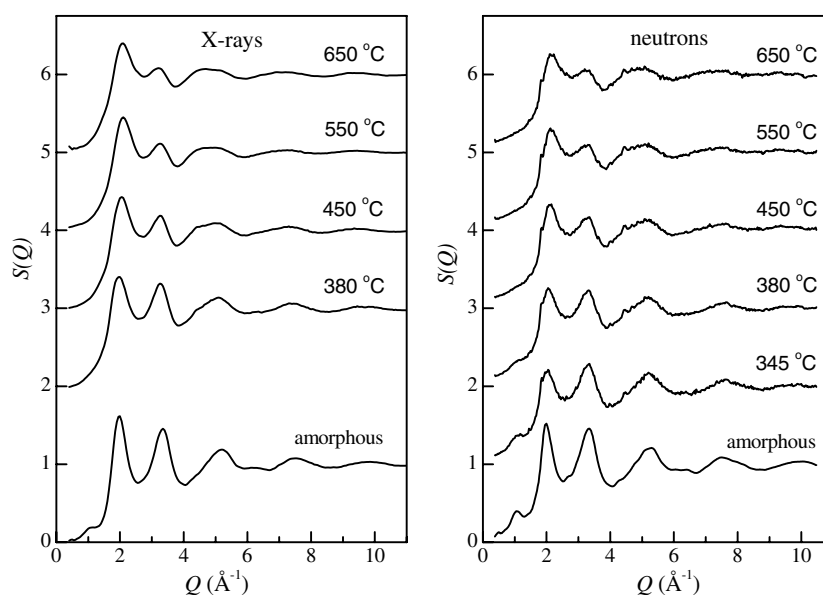


Figure 1. Experimental structure factors of $\text{Ge}_{15}\text{Te}_{85}$ alloys.

corrections and normalization to a vanadium standard, which were done with the CORRECT program described in [24].

X-ray diffraction experiments were carried out at the BW5 experimental station [25] at HASYLAB, DESY. The samples were filled and sealed into quartz capillaries of 2 mm in diameter and with wall thickness of about 0.02 mm. The energy of the radiation was 125 keV. The scattered intensity was measured between 0.4 and 20 \AA^{-1} . Statistical error at the tail of the curve was less than 0.2%. Raw data were corrected for detector dead-time, background, polarization, absorption, and variations in detector solid angle.

3. Experimental results

The neutron diffraction measurements on the $\text{Ge}_{15}\text{Te}_{85}$ alloy were performed in the liquid state up to $740 \text{ }^\circ\text{C}$ and in the supercooled state at $345 \text{ }^\circ\text{C}$. The x-ray scattering curves of liquid $\text{Ge}_{15}\text{Te}_{85}$ were recorded at 380 , 450 , 550 and $650 \text{ }^\circ\text{C}$. Attempts to supercool the liquid sample melted with a light-spot heater at the BW5 synchrotron station were unsuccessful. The experimental structure factors of liquid and amorphous (redrawn from [26]) $\text{Ge}_{15}\text{Te}_{85}$ are shown in figure 1. $\text{Ge}_{25}\text{Te}_{75}$ and $\text{Ge}_{33}\text{Te}_{67}$ alloys were measured at 550 and $750 \text{ }^\circ\text{C}$ respectively; the structure factors are shown in figure 2.

The shape of the experimental structure factors depends on the temperature as well as on the composition of the alloys. It is seen from figure 3 that the height of the first, $S(Q^I)$, and the second, $S(Q^{II})$, maximum for the $\text{Ge}_{15}\text{Te}_{85}$ alloy exhibit strong but different temperature dependences: $S(Q^I)$ at first increases when the temperature rises up to 450 – $550 \text{ }^\circ\text{C}$, and then decreases at $650 \text{ }^\circ\text{C}$; $S(Q^{II})$ decreases continuously with increasing temperature. It is to be mentioned that the density of $\text{Ge}_{15}\text{Te}_{85}$ changes non-monotonically above the melting point with a maximum close to $500 \text{ }^\circ\text{C}$ [8, 9]. Such an anomalous temperature behaviour of the density and the intensity of the first maximum in the $S(Q)$ of liquid $\text{Ge}_{15}\text{Te}_{85}$ should be reflected by some structural changes in the short-range order. Bergman *et al* [20] assign the

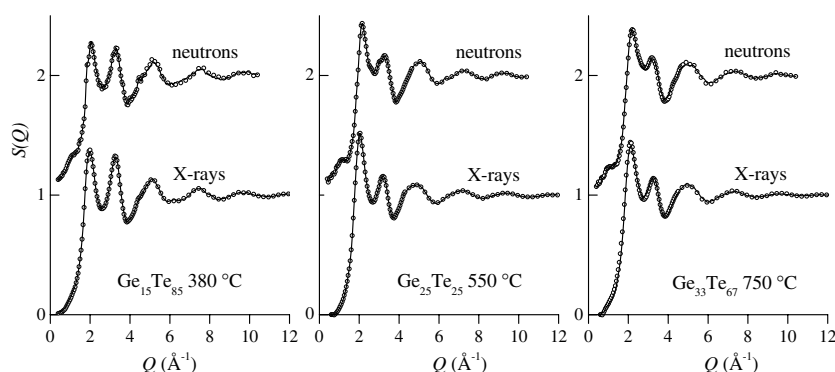


Figure 2. Experimental (circles) and RMC simulated (lines) structure factors of liquid $\text{Ge}_{15}\text{Te}_{85}$, $\text{Ge}_{25}\text{Te}_{75}$ and $\text{Ge}_{33}\text{Te}_{67}$. Just every fifth experimental point is shown for $Q > 4.5 \text{ \AA}^{-1}$ for clarity. Simulation constraints: $\text{Ge}_{15}\text{Te}_{85}$ — $N_{\text{GeGe}} = 0$; $r_{\text{TeTe}} = 2.5 \text{ \AA}$; $r_{\text{GeTe}} = 2.3 \text{ \AA}$; $r_{\text{GeGe}} = 3.5 \text{ \AA}$; $\text{Ge}_{25}\text{Te}_{75}$ — $N_{\text{GeGe}} = 0.6$; $r_{\text{TeTe}} = 2.5 \text{ \AA}$; $r_{\text{GeTe}} = 2.3 \text{ \AA}$; $r_{\text{GeGe}} = 3.5 \text{ \AA}$; $\text{Ge}_{33}\text{Te}_{67}$ — $N_{\text{GeGe}} = 0.6$; $r_{\text{TeTe}} = 2.5 \text{ \AA}$; $r_{\text{GeTe}} = 2.3 \text{ \AA}$; $r_{\text{GeGe}} = 2.3 \text{ \AA}$.

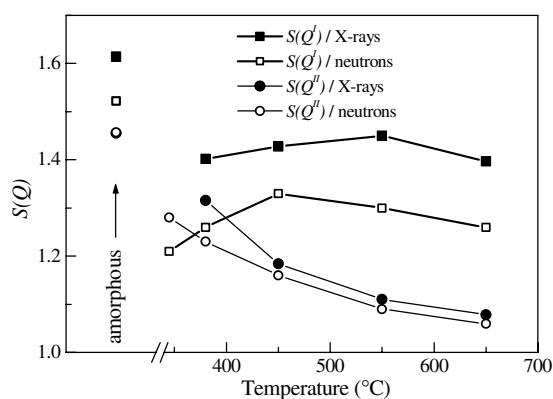


Figure 3. Temperature dependences of $S(Q^I)$ and $S(Q^{II})$ for the $\text{Ge}_{15}\text{Te}_{85}$ alloy.

changes of $S(Q)$ to an increase of the number of Te neighbours around Ge atoms. In their analysis they do not consider the possible changes of Te–Te correlations. Taking into account that pure liquid Te exhibits similar anomalous behaviour (see e.g. figures 1–3 of [20]) this simplification may limit the validity of their argumentation. In our opinion it is not possible to determine what exactly has changed in the SRO of binary Ge–Te alloys only from the total structure factors or pair distribution functions. Therefore further analysis will be carried out on the partial functions derived with the help of RMC.

4. RMC simulations

Since the first publication on the reverse Monte Carlo technique [21], it has been illustrated in a number of studies that RMC is a useful tool for modelling of the atomic structure of non-crystalline substances and determination of the partial pair correlation functions and other structural parameters (for details of the technique the reader is referred to a comprehensive review of McGreevy [22]). Recently we have proven that reliable partial structure factors and partial pair correlation functions of a binary liquid alloy can be obtained with two independent diffraction curves if additional physical information (e.g. atomic size differences

Table 1. The x-ray W_{ij}^X (at $Q = 0$) and neutron W_{ij}^N weights of the partial structure factors for the investigated Ge–Te alloys.

Composition	W_{TeTe}^X	W_{TeTe}^N	W_{GeTe}^X	W_{GeTe}^N	W_{GeGe}^X	W_{GeGe}^N
Ge ₁₅ Te ₈₅	0.814	0.641	0.176	0.319	0.010	0.040
Ge ₂₅ Te ₇₅	0.689	0.464	0.282	0.434	0.029	0.102
Ge ₃₃ Te ₆₇	0.589	0.344	0.357	0.485	0.054	0.171

or coordination constraints) can be built into the simulation [27]. Due to different values of the x-ray atomic scattering factors ($f_{\text{Ge}}(0) = 32$ e.u., $f_{\text{Te}}(0) = 52$ e.u.) and the neutron scattering lengths ($b_{\text{Ge}} = 8.185$ fm, $b_{\text{Te}} = 5.8$ fm [28]) for Ge and Te and application of plausible physical constraints one may expect to obtain a reliable picture of the atomic distribution in Ge–Te alloys.

In the present work, coupled simulations of the x-ray and neutron diffraction measurements were carried out with boxes of 15 000–20 000 atoms. The densities of liquid alloys were taken from [20, 29]. Initial configurations were obtained by hard sphere simulation runs, i.e. fitting no experimental data but applying hard sphere cut-offs and coordination constraints. For all compositions the cut-off distances between Ge–Te and Te–Te pairs were 2.3 and 2.5 Å respectively. For Ge₁₅Te₈₅, Ge–Ge bonding was eliminated by setting the minimum distance r_{GeGe} to 3.5 Å. In the case of Ge₃₃Te₆₇ and Ge₂₅Te₇₅ alloys, runs with $r_{\text{GeGe}} = 2.3$ Å were also carried out. In these runs Ge–Ge coordination constraints were also applied by restricting the average Ge–Ge coordination number between 2.3 and 3.2 Å.

As an example, the RMC simulated and experimental total structure factors for liquid Ge₁₅Te₈₅ (380 °C), Ge₂₅Te₇₅ (550 °C) and Ge₃₃Te₆₇ (750 °C) are plotted in figure 2. The agreement between the experimental $S_{X,N}^{\text{exp}}$ and the simulated $S_{X,N}^{\text{RMC}}$ structure factors was judged by the value of

$$\chi_{X,N}^2 = \frac{\sum_i (S_{X,N}^{\text{RMC}}(Q_i) - S_{X,N}^{\text{exp}}(Q_i))^2}{\sigma_{X,N}^2} \quad (1)$$

where σ is a parameter of RMC chosen appropriately to determine the ratio of accepted moves. Subscripts X and N refer to x-ray or neutron diffraction data. The value of σ was usually between 0.0015 and 0.003, depending on the temperature and composition. However, it was always kept constant when χ^2 was investigated as the function of the coordination constraints. The maximum random atomic displacement was 0.2 Å and the ratio of accepted moves was usually between 0.2 and 0.4.

5. Discussion

5.1. Ge₁₅Te₈₅ eutectic alloy

The partial structure factors and pair distribution functions for liquid Ge₁₅Te₈₅ simulated with RMC are shown in figure 4. On the basis of Raman scattering data we assumed in our previous paper [26] that there are no Ge–Ge bonds in amorphous Ge₁₅Te₈₅. It is reasonable to assume that this also holds for liquid Ge₁₅Te₈₅ in the vicinity of the melting point. The existence of the Ge–Ge bonds cannot be ruled out at elevated temperatures. The weight of the Ge–Ge partial structure factor is so small that for this composition the diffraction measurements are not conclusive concerning the existence of the Ge–Ge bonds. This is clearly seen from table 1 where the weights of the partial structure factors for the alloys studied are given.

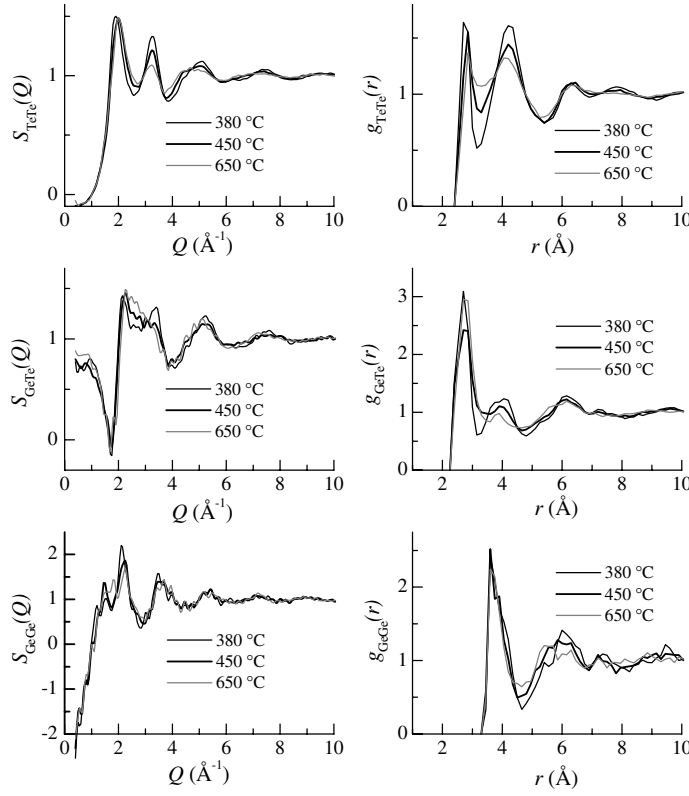


Figure 4. Temperature evolution of the RMC-simulated partial structure factors and partial pair correlation functions of liquid $\text{Ge}_{15}\text{Te}_{85}$.

Table 2. The nearest neighbour distances r_{ij} and coordination numbers N_{ij} for amorphous and liquid $\text{Ge}_{15}\text{Te}_{85}$.

Temperature	r_{TeTe} (Å)	r_{GeTe} (Å)	N_{TeTe}	N_{GeTe}	N_{TeX}
Amorphous ^a	2.73	2.62	1.62	3.95	2.32
380 °C	2.75	2.70	1.7	3.7	2.4
450 °C	2.85	2.77	1.9	4.0	2.6
550 °C	2.88	2.82	1.9	4.0	2.6
650 °C	2.83	2.77	1.9	4.6	2.7

^a [28] (XRD + ND + RMC, ‘tetrahedral’ model).

The partial structure factors and pair distribution functions are strongly temperature dependent (figure 4). At 380 °C (just above melting) both $g_{\text{TeTe}}(r)$ and $g_{\text{GeTe}}(r)$ have a distinct first minimum; Te–Te and Ge–Te coordination numbers are 1.7 and 3.7 respectively. At elevated temperatures the first minimum of $g_{\text{TeTe}}(r)$ becomes more and more shallow and the overlap between the first and second coordination spheres is stronger. The differences between the partial pair distribution functions at 550 and 650 °C are small and the data for 550 °C are therefore not shown in figure 4. The nearest neighbour distances r_{ij} and coordination numbers N_{ij} for all temperatures calculated up to the first minimum of $r^2 g_{\text{TeTe}}(r)$ are given in table 2.

From the temperature evolution of the Te–Te and Ge–Te partial pair correlation functions and coordination parameters (figure 4 and table 2) it is seen that, in accordance with the physico-chemical properties, the temperature induced structural changes in liquid $\text{Ge}_{15}\text{Te}_{85}$ are very pronounced in the temperature interval from $\vartheta_{\text{cut}} = 375$ °C up to 450 °C, and they

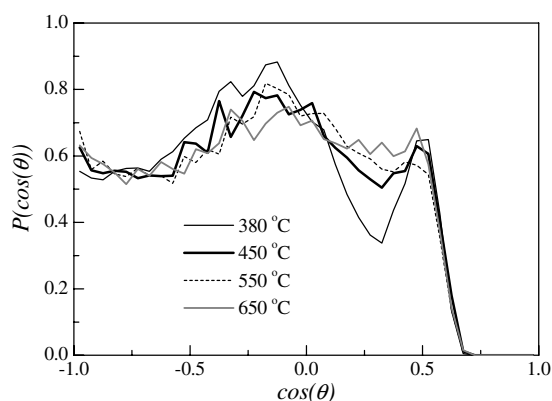


Figure 5. Te–Ge–Te bond angle distribution in liquid $\text{Ge}_{15}\text{Te}_{85}$ in dependence on temperature.

Table 3. The nearest neighbour distances r_{ij} and coordination numbers N_{ij} for liquid $\text{Ge}_{25}\text{Te}_{75}$ at 550 °C and $\text{Ge}_{33}\text{Te}_{67}$ at 750 °C.

Alloy	r_{TeTe} (Å)	r_{GeTe} (Å)	r_{GeGe} (Å)	N_{TeTe}	N_{GeTe}	N_{GeGe}
$\text{Ge}_{25}\text{Te}_{75}$	3.10	2.81	2.5	2.1	4.2	0.5 ^a
$\text{Ge}_{33}\text{Te}_{67}$	2.81	2.81	2.9	0.8	4.1	0.6 ^a

^a These values were applied as the constraints in RMC simulations.

are not so strong at higher temperatures. It can also be observed that there is a slight increase in the Ge–Te coordination number and Ge–Te nearest distance. The changes of the respective values for the Te–Te pairs are comparable. As pure elemental Te shows a similar behaviour in the supercooled region [30], our results suggest that the addition of Ge stabilizes the low-temperature structure of liquid Te and the structural transformations of the eutectic $\text{Ge}_{15}\text{Te}_{85}$ alloy cannot be assigned only to changes in $g_{\text{GeTe}}(r)$ as suggested in [20].

Figure 5 gives the Te–Ge–Te bond angle distribution for the liquid $\text{Ge}_{15}\text{Te}_{85}$ derived with the help of RMC. A striking feature is the usual artificial peak at 60°. Apart from this, it can be concluded that the bond angle distribution has a maximum around 100°, which is broadened with increasing temperature. This suggests that with increasing temperatures tetrahedral local order transforms to a more dense atomic arrangement. This is in line with conclusions made by Bergman *et al* [20] on the basis of neutron diffraction and density measurements in liquid $\text{Ge}_{15}\text{Te}_{85}$.

5.2. $\text{Ge}_{25}\text{Te}_{75}$ alloy

The structure of liquid $\text{Ge}_{25}\text{Te}_{75}$ was modelled in a series of the simulation runs where the number of Ge–Ge neighbours was varied. Figure 6 shows the partial structure factors and partial pair distribution functions of liquid $\text{Ge}_{25}\text{Te}_{75}$ at 550 °C obtained with different values of the Ge–Ge coordination number ($N_{\text{GeGe}} = 0$, $N_{\text{GeGe}} = 0.6$ and $N_{\text{GeGe}} = 1.0$). It has been found that for $N_{\text{GeGe}} < 1.6$ the quality of the fit was not so sensitive to the number of Ge–Ge pairs as in the case of $\text{Ge}_{33}\text{Te}_{67}$ (this will be seen later). It can also be observed that changes in $g_{\text{GeGe}}(r)$ and $g_{\text{GeTe}}(r)$ compensate each other. From the shape of the first peak in $g_{\text{GeGe}}(r)$ it appears that N_{GeGe} should not be higher than 0.8–1 for the $\text{Ge}_{25}\text{Te}_{75}$ composition. The values of the nearest neighbours and the coordination numbers for liquid $\text{Ge}_{25}\text{Te}_{75}$ at 550 °C estimated with the constraint $N_{\text{GeGe}} = 0.6$ are given in table 3. It should however be mentioned that the first coordination shell in $g_{\text{TeTe}}(r)$ is not well defined on the right-hand side.

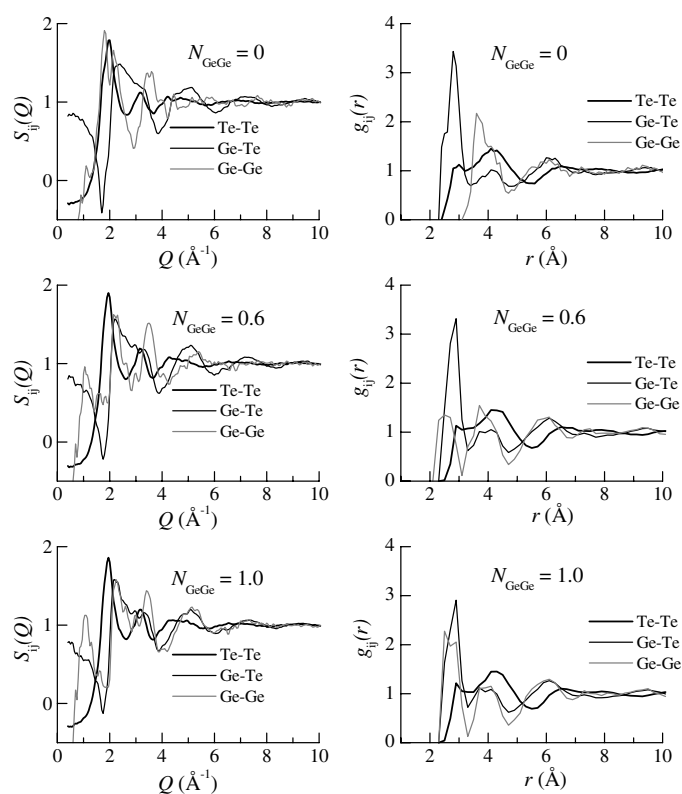


Figure 6. Partial pair distribution functions of liquid $\text{Ge}_{25}\text{Te}_{75}$ at $550\text{ }^{\circ}\text{C}$ simulated with different values of N_{GeGe} .

The Te–Ge–Te bond angle distribution for the liquid $\text{Ge}_{25}\text{Te}_{75}$ was also determined from the simulation. This result will be discussed together with the respective data for the $\text{Ge}_{33}\text{Te}_{67}$ composition.

5.3. $\text{Ge}_{33}\text{Te}_{67}$ alloy

GeX_2 ($X = \text{S}, \text{Se}, \text{Te}$) glasses and melts belong to the most intensely investigated disordered systems. Maruyama *et al* studied liquid Ge–chalcogen mixtures by time of flight neutron diffraction [31]. In works [32–34] the structure of amorphous and liquid GeSe_2 was investigated by neutron diffraction with isotopic substitution. It was found that both states comprise edge- and corner-sharing tetrahedral units. It was also shown that 25(5)% of Ge and 20(5)% of Se atoms are involved in homopolar bonds. While Ge–Se melts can be vitrified up to at least 40 at.% Ge content [35] Ge–Te glasses can be obtained only in the vicinity of the eutectic point (15 at.% Ge), where the melt can be deeply supercooled. Though a detailed and in depth explanation of this phenomenon is certainly far beyond the scope of our paper, two remarks can be made here: (i) there are two stable crystalline compounds (GeSe and GeSe_2) in the $\text{Ge}_x\text{Se}_{1-x}$ system. The existence of competing crystal structures may enhance the glass-forming ability (especially for $x \geq 1/3$); (ii) it has been shown [36] that there are no Ge–Ge bonds in vitreous $\text{Ge}_x\text{Te}_{1-x}$ ($0.16 \leq x \leq 0.20$). Therefore, it can be concluded that in contrast with the Ge–Se system the formation of Ge–Ge bonds is not favourable in Ge–Te glasses. This is also supported by the fact that upon solidification liquid $\text{Ge}_x\text{Te}_{1-x}$ ($x < 0.5$) alloys segregate into two phases (GeTe and Te) without Ge–Ge bonds.

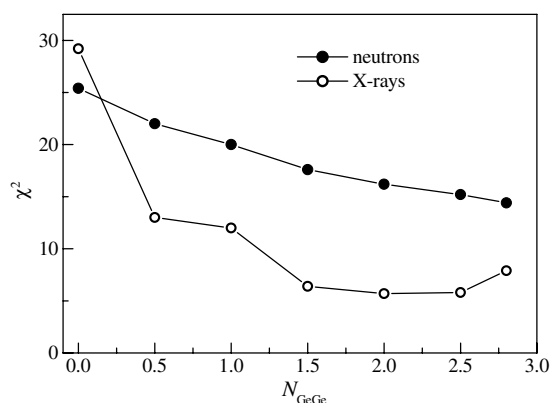


Figure 7. Dependence of the fit quality χ^2 for liquid $\text{Ge}_{33}\text{Te}_{67}$ at 750°C on the constraint N_{GeGe} .

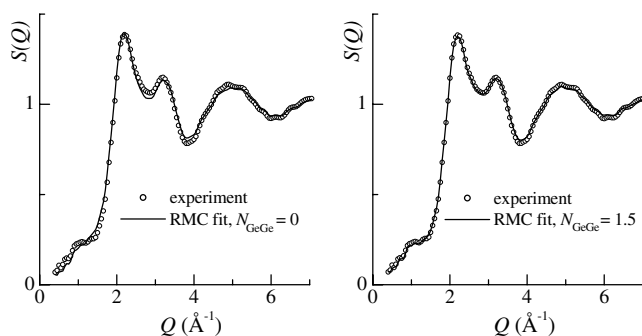


Figure 8. The experimental neutron structure factor of liquid $\text{Ge}_{33}\text{Te}_{67}$ at 750°C and the structure factors simulated with $N_{\text{GeGe}} = 0$ and $N_{\text{GeGe}} = 1.5$.

Several different simulation runs were carried out to study the structure of liquid $\text{Ge}_{33}\text{Te}_{67}$. It has been found that the diffraction data cannot be well fitted if a large minimum Ge–Ge distance ($r_{\text{GeGe}} = 3.5 \text{ \AA}$) is assumed, i.e. when Ge–Ge bonds are excluded. The fit was significantly improved when the minimum Ge–Ge distance was set to be 2.3 \AA and the average Ge–Ge coordination number was raised to 1.5–2: the χ^2 value (equation (1)) for x-ray data decreased by about 70–80% (see figure 7). Parts of the experimental neutron structure factor for liquid $\text{Ge}_{33}\text{Te}_{67}$ and the structure factors simulated with $N_{\text{GeGe}} = 0$ and $N_{\text{GeGe}} = 1.5$ are compared in figure 8. It is noteworthy that the sum of Ge–Ge and Ge–Te coordination numbers remained about 4.8 ± 0.2 in all cases. Regardless of the constraints used in RMC (coordination numbers or nearest neighbour distances), the Ge–Te bond length was about 2.85 \AA for the liquid $\text{Ge}_{33}\text{Te}_{67}$.

However, it appears that the Ge–Ge coordination number of 1.5–2 is too high for this composition. This is quite close to the value which would be obtained for the random distribution of Ge and Te atoms (i.e. when one-third of the neighbours of Ge atoms are other Ge atoms). Moreover, when we applied the constraint $N_{\text{GeGe}} \geq 1$ then artificial sharp features appeared on the Ge–Ge partial pair distribution functions. Therefore, we assume that the real number of Ge–Ge atoms is smaller, and $N_{\text{GeGe}} = 0.6$ is chosen for a further analysis. The RMC simulated (with $N_{\text{GeGe}} = 0.6$) and experimental total structure factors for the liquid $\text{Ge}_{33}\text{Te}_{67}$ are compared in figure 2. The respective partial structure factors and pair distribution functions are plotted in figure 9.

It is noteworthy that in comparison with liquid $\text{Ge}_{25}\text{Te}_{75}$ the first and the second maxima in the Te–Te pair distribution function shift to lower r -values and become slightly sharper (see figure 10 and table 3). This suggests that the structure becomes more compact in the latter

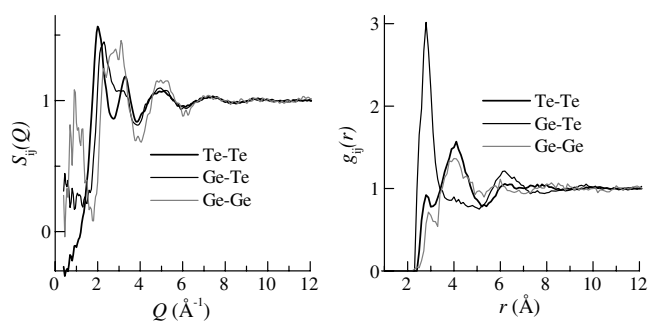


Figure 9. Partial structure factors and partial pair correlation functions of liquid $\text{Ge}_{33}\text{Te}_{67}$ at 750°C (simulated with $N_{\text{GeGe}} = 0.6$).

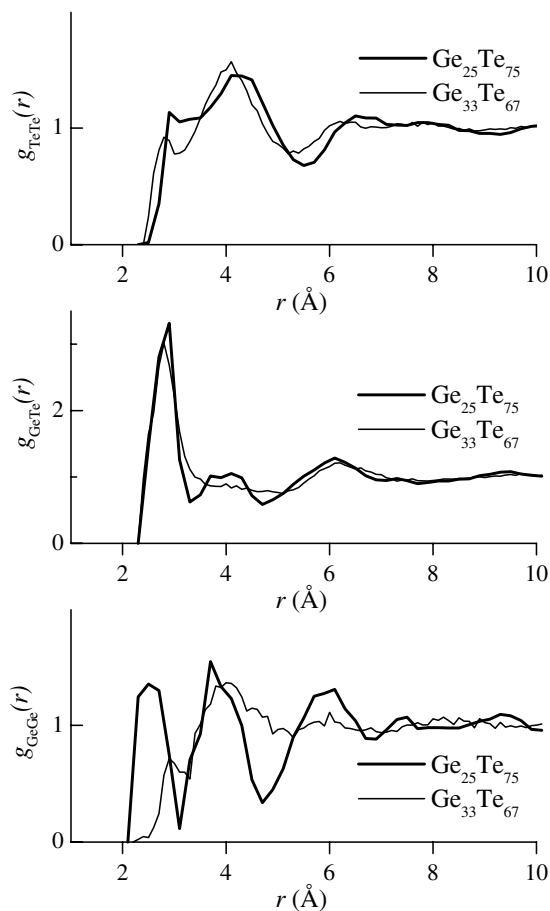


Figure 10. Comparison of the RMC-simulated partial pair distribution functions for liquid $\text{Ge}_{25}\text{Te}_{75}$ and $\text{Ge}_{33}\text{Te}_{67}$ alloys.

case. The first maximum in the Ge–Te pair distribution function for liquid $\text{Ge}_{33}\text{Te}_{67}$ is virtually unchanged as compared to that of liquid $\text{Ge}_{25}\text{Te}_{75}$. But the second maximum in the $g_{\text{GeTe}}(r)$ for liquid $\text{Ge}_{33}\text{Te}_{67}$ is smeared out in comparison with liquid $\text{Ge}_{25}\text{Te}_{75}$. These changes are obviously related to an increased Ge concentration. There seems to be a tendency of reducing the number of Te–Te bonds.

A formation of Ge–Ge bonds in liquid $\text{Ge}_{33}\text{Te}_{67}$ was also found in the EXAFS study of Hosokawa *et al* [37]. They reported 3.2–3.25 Å both for the Ge–Ge and Ge–Te bond lengths in liquid GeTe_2 at 700°C . These distances are remarkably longer than those determined by us

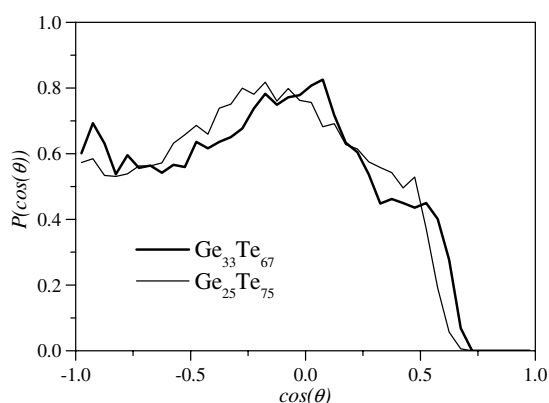


Figure 11. Te–Ge–Te bond angle distribution in liquid $\text{Ge}_{25}\text{Te}_{75}$ at 550°C and $\text{Ge}_{33}\text{Te}_{67}$ at 750°C .

(2.9 \AA and 2.81 \AA respectively). It is not clear where the differences originate. However, as we have already mentioned it was not possible to fit the experimental data using RMC with the constraint $r_{\text{GeGe}} > 3 \text{ \AA}$. Taking into account rather high weights of Ge–Te partials both in x-ray and neutron diffraction patterns (table 1), the reliability of the nearest neighbour distances derived with RMC is also very high. It should also be mentioned that the useful EXAFS data range in [37] only extends up to $7\text{--}8 \text{ \AA}^{-1}$. As the XANES region extends up to $3\text{--}4 \text{ \AA}^{-1}$, it remains to be seen how accurately these values could be determined on the basis of such a limited data range.

The Te–Ge–Te bond angle distribution in liquid $\text{Ge}_{25}\text{Te}_{75}$ and $\text{Ge}_{33}\text{Te}_{67}$ derived with RMC are shown in figure 11. Except for the artificial peak at about 60° , which often appears in configurations obtained with RMC, the following features should be noted: (i) there is a maximum in the Te–Ge–Te bond angle distribution for liquid $\text{Ge}_{25}\text{Te}_{75}$ at about 100° ; (ii) the maximum position in the Te–Ge–Te bond angle distribution for liquid $\text{Ge}_{33}\text{Te}_{67}$ is situated at about 90° . These findings suggest that the atomic packing is more compact in liquid $\text{Ge}_{33}\text{Te}_{67}$ as compared to $\text{Ge}_{25}\text{Te}_{75}$ alloy, as already concluded from the analysis of the Te–Te and Ge–Te nearest neighbour distances. The shift of the peak in the bond angle distribution curve to 90° and the appearance of the maximum at $\sim 160^\circ$ for liquid $\text{Ge}_{33}\text{Te}_{67}$ give evidence of a structural transformation from tetrahedral towards octahedral local ordering with increasing Ge content.

6. Summary

- (1) There are significant differences in the local atomic order of liquid $\text{Ge}_{15}\text{Te}_{85}$ at low temperatures up to about 450°C including the supercooled liquid state and at the temperatures above 450°C . The structural transformations of the $\text{Ge}_{15}\text{Te}_{85}$ alloy are connected with the changes both in $g_{\text{GeTe}}(r)$ and $g_{\text{TeTe}}(r)$.
- (2) It is assumed that there are no Ge–Ge bonds in liquid $\text{Ge}_{15}\text{Te}_{85}$ close to the melting point but they may exist at higher temperatures. It follows from the analysis of the experimental data that Ge–Ge bonding appears when Ge content is increased. Thus Ge–Ge bonding seems to be present in liquid $\text{Ge}_{25}\text{Te}_{75}$ and $\text{Ge}_{33}\text{Te}_{67}$.
- (3) It can be assumed that the temperature at which the structural changes in the Te-rich Ge–Te alloys occur is related to their Ge content. Indeed, taking into account the composition and temperature dependences of the density, sound velocity and other physical properties of liquid Te and Ge–Te alloys [29, 30] and the results of our structural investigations it can be concluded that addition of Ge (up to about 15–20 at.% Ge) to Te stabilizes the low-temperature liquid structure.

- (4) We assume that there is a connection between the glass-forming ability of Ge–Te alloys and Ge–Ge/Ge–Te bonding. It is probable that a higher number of Ge–Te bonds stabilizes the low temperature liquid structure and for the alloys with a high glass-forming ability (around Ge₁₅Te₈₅ composition) the liquid–liquid phase transformations take place above the liquidus line. On the other hand, a high number of Ge–Ge bonds is not favourable in the Te-rich Ge–Te alloys. This is also supported by the fact that upon solidification liquid Ge–Te alloys segregate into two phases—GeTe and Te—without Ge–Ge bonds.

Acknowledgments

This work has been supported by the European Community—Access to Research Infrastructure action of the Improving Human Potential Programme, contract No HPRI-CT 2001-00127. PJ was supported by the OTKA (Hungarian Basic Research Fund) grant No T048580.

References

- [1] Joffe A F and Regel A R 1960 *Prog. Semicond.* **4** 237
- [2] Glazov V M, Chizhevskaja S N and Glagoleva N N 1967 *Liquid Semiconductors* (Moscow: Nauka)
- [3] Cutler M 1977 *Liquid Semiconductors* (New York: Academic)
- [4] Legendre B and Hancheng C 1984 *Thermochim. Acta* **78** 141
- [5] *Physical Chemistry* 1996 (*Landolt-Börnstein New Series* vol 5F Group IV) (Berlin: Springer) <http://www.springeronline.com>
- [6] Moore A G, Maghrabi C and Parker J M 1978 *J. Mater. Sci. Lett.* **13** 1127
- [7] Valiant J C and Faber T E 1974 *Phil. Mag.* **29** 571
- [8] Tsuchiya Y 1993 *J. Non-Cryst. Solids* **156–158** 704
- [9] Tsuchiya Y 2002 *J. Non-Cryst. Solids* **312–314** 212
- [10] Tschirner H-U, Pazdrič I P and Weikart R 1983 *Wiss. Z. Tech. Hochsch. Karl-Marx-Stadt* **25/2** 219
- [11] Tschirner H-U, Born Th, Neumann H, Hoyer W and Wobst M 1986 *Wiss. Z. Tech. Hochsch. Karl-Marx-Stadt* **28/2** 249
- [12] Herwig F and Wobst M 1991 *Z. Metallk.* **82** 917
- [13] Terzieff P, Komarek K L and Wachtel E 1986 *Phys. Chem. Liq.* **15** 217
- [14] Neumann H, Matz W, Hoyer W and Wobst M 1985 *Phys. Status Solidi a* **90** 489
- [15] Neumann H, Hoyer W, Matz W and Wobst M 1987 *J. Non-Cryst. Solids* **97/98** 1251
- [16] Nicotera E, Corchia M, Giorgi G De, Villa F and Antonini M 1973 *J. Non-Cryst. Solids* **11** 417
- [17] Kameda Y, Uemura O and Usuki T 1996 *Mater. Trans. JIM* **37/11** 1655
- [18] Yoshioka S, Kawakita Y, Kanehira M and Takeda S 1999 *Japan. J. Appl. Phys. Suppl.* **38-1** 468
- [19] Bichara C, Gaspard J P and Raty J-R 2002 *J. Non-Cryst. Solids* **312–314** 341
- [20] Bergman C, Bichara C, Gaspard J P and Tsuchiya Y 2003 *Phys. Rev. B* **67** 104202
- [21] McGreevy R L and Pusztai L 1988 *Mol. Simul.* **1** 359
- [22] McGreevy R L 2001 *J. Phys.: Condens. Matter* **13** R877
- [23] Wannberg A, Mellergård A, Zetterström P, Delaplane R, Grönros M, Karlsson L-E and McGreevy R L 1999 *J. Neutron Res.* **8** 133
- [24] Howe M A, McGreevy R L and Zetterström P 1996 *CORRECT: A Correction Program for Neutron Diffraction Data (NFL Studsvik Internal Report)* <ftp://www.studsvik.uu.se/pub/correct/>
- [25] Poulsen H, Neuefeind J, Neumann H B, Schneider J R and Zeidler M D 1995 *J. Non-Cryst. Solids* **188** 63
- [26] Jóvári P, Kaban I, Hoyer W, Delaplane R G and Wannberg A 2005 *J. Phys.: Condens. Matter* **17** 1529
- [27] Kaban I, Gruner S, Hoyer W, Jóvári P, Delaplane R G and Wannberg A 2005 *Phys. Chem. Glasses* **46/4** 472
- [28] Sears V F 1992 *Neutron News* **3** 26
- [29] Tsuchiya Y 1991 *J. Phys. Soc. Japan* **60** 227
- [30] Tsuzuki T, Yao M and Endo H 1995 *J. Phys. Soc. Japan* **64** 485
- [31] Maruyama K, Ebata H, Suzuki S, Misawa M, Takeda S and Kawakita Y 1999 *J. Non-Cryst. Solids* **250–252** 483
- [32] Penfold I T and Salmon P S 1991 *Phys. Rev. Lett.* **67** 97
- [33] Petri I, Salmon P S and Fischer H E 2000 *Phys. Rev. Lett.* **84** 2413
- [34] Salmon P S and Petri I 2003 *J. Phys.: Condens. Matter* **15** S1509
- [35] Borisova Z U 1981 *Glassy Semiconductors* (New York: Plenum) p 104
- [36] Uemura O, Hayasaka N, Tokairin S and Usuki T 1996 *J. Non-Cryst. Solids* **205–207** 189
- [37] Hosokawa S, Tamura K, Inui M and Endo H 1993 *J. Non-Cryst. Solids* **156–158** 712